



Cite this: *Chem. Sci.*, 2025, **16**, 20382

All publication charges for this article have been paid for by the Royal Society of Chemistry

Received 26th June 2025
 Accepted 13th September 2025
 DOI: 10.1039/d5sc04733a
rsc.li/chemical-science

Introduction

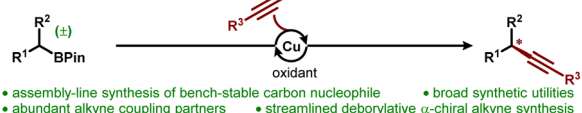
Alkylboronic pinacol esters have emerged as highly versatile reagents in organic synthesis.^{1–5} Their capacity for iterative homologation through 1,2-boronate rearrangement allows for efficient and stereocontrolled assembly of complex frameworks.^{6–9} The unique stability and reactivity of α -borylcarbanions render them readily accessible intermediates for alkyl skeleton construction.^{10–15} Despite their synthetic potentials imparted by the vacant boron p orbital, the application of alkylboronic pinacol esters in asymmetric deborylative C–C cross-coupling remains limited due to sluggish transmetalation and competing protodeboronation pathways.¹⁶ In particular, an enantioconvergent deborylative alkynylation protocol could unlock powerful synthetic disconnections by combining the modularity of alkylboronic pinacol esters and versatility of alkynyl groups (Fig. 1A)—yet such a transformation remains elusive. Seminal work by Aggarwal¹⁷ and Morken¹⁸ (Fig. 1B) demonstrated the potential of enantioenriched alkylboronic pinacol esters for α -chiral alkyne synthesis *via* (1) enantioselective Zweifel-type alkenylations followed by 1,2-elimination, and (2) stereoretentive transmetalation to CuCN facilitated by alkyl lithium reagents and subsequent coupling with alkynyl bromides, respectively. We reasoned that an alternative enantioconvergent strategy, which directly engages racemic alkylboronic pinacol esters with readily available terminal alkynes, could provide a streamlined approach to these valuable products. We herein disclose the first enantioconvergent

Cu-catalyzed enantioconvergent deborylative alkynylation

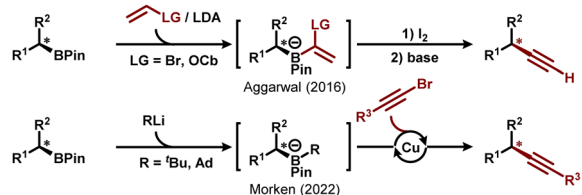
Joshua F. Head, Tanner J. Schubert, Biyu Zhao and Yuyang Dong  *

Alkylboronic pinacol esters represent a highly attractive class of reagents due to their modular synthesis and unique reactivity conferred by the vacant boron p-orbital. However, their direct application in asymmetric C–C cross-coupling reactions remains underexplored. Herein, we report a Cu-catalyzed deborylative strategy to access α -chiral alkynes that delivers good enantioselectivity and accommodates a broad range of functional groups and heterocycles. The reaction is proposed to proceed through a radical-relay pathway: an aminal radical-mediated C–B bond cleavage followed by Cu-catalyzed asymmetric alkynylation. The reaction mechanism was probed using a combination of radical clock ring-opening study, radical trapping experiments, and enantioconvergence test with enantioenriched starting materials. Density functional theory (DFT) calculations demonstrate the feasibility of a Cu-mediated inner-sphere C–C bond-forming pathway and attribute the observed enantioselectivity to attractive ligand–substrate halogen– π interactions.

A. Cu-catalyzed enantioconvergent deborylative cross-coupling to access α -chiral alkynes



B. Previous work: Stereospecific deborylative alkynylation using enantioenriched alkylboron reagents



C. This work: Direct asymmetric coupling of racemic alkylboronic pinacol esters and terminal alkynes

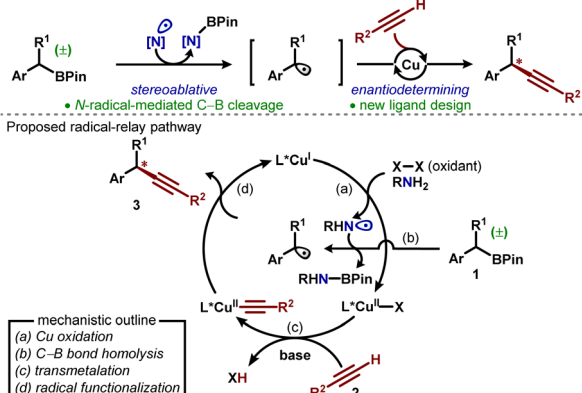


Fig. 1 (A) A Cu-catalyzed asymmetric deborylative cross-coupling approach to α -chiral alkyne synthesis; (B) stereospecific transformations as the only examples of deborylative protocols to access α -chiral alkynes; (C) employing alkylboronic pinacol esters in enantioconvergent alkynylation through single-electron processes.



deborylation alkynylation protocol facilitated by ligand design and proceeding through a Cu-catalyzed radical relay.^{19–21}

We envisioned that this transformation could be achieved through two key mechanistic steps (Fig. 1C): (1) the homolytic cleavage of C–B bonds and (2) the asymmetric functionalization of alkyl radicals *via* Cu(II) alkynyl intermediates.^{22–31} The single-electron activation of alkylboronic pinacol esters is often hindered by their high oxidation potential.^{32–34} We previously overcame this challenge by employing an *in situ* generated aminyl radical to promote C–B bond homolysis through an inner-sphere pathway.^{34–36} Following the C–B bond activation (steps a–b), we propose that the resulting prochiral radical engages an *in situ* generated Cu(II) bisalkynyl intermediate, yielding the optically active product (steps c and d). We anticipate that potential complications with this approach involve (1) homocoupling of terminal alkynes and (2) undesired C–N coupling with amine activator. We further reasoned that these challenges could be circumvented through the judicious choice of base additives and oxidants to balance the relative rates among alkyne transmetalation, C–B bond activation, and radical functionalization steps. We herein report the successful implementation of this strategy for an enantioconvergent deborylative alkynylation protocol and the corresponding mechanistic studies to guide our future expansion of this C–C cross-coupling platform.

Results and discussion

Reaction optimization

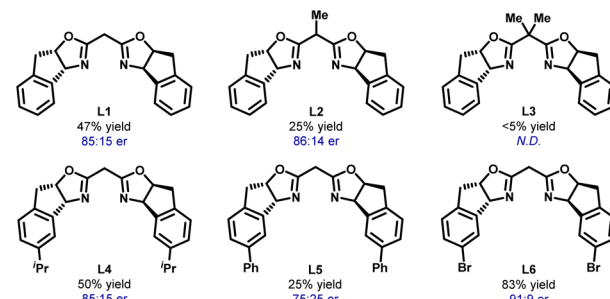
We initiated our investigation by examining the cross-coupling between alkylboronic pinacol ester **1a** and 2-ethynylthiophene **2a**. We tested a range of copper sources, chemical oxidants, amine additives, external bases, and reaction solvents (See SI, Table S1 for full optimization details). The focus on inda(box)-type ligands (box: bisoxazoline) was motivated by the pioneering work of Liu *et al.*,^{20–23} who demonstrated their utility in asymmetric radical alkynylation. A combination of cuprous trifluoromethanesulfonate benzene complex and parent inda-(box) ligand **L1** yielded product **3a** with moderate yield and enantioselectivity (Table 1). We identified two potential strategies to improve the reaction selectivity: (1) tuning the ligand bite-angle *via* *meso*-substitution³⁷ and (2) enhancing ligand-substrate interactions by installing distal substituents.^{38–40} While introducing methyl (**L2–L3**) or other groups (Table S1) to the *meso*-position diminished the reaction yield,⁴¹ modifications at the phenyl *meta*-position (**L4–L6**) proved effective. In particular, bromine substitution in **L6** delivered the highest yield and enantioselectivity. We attributed this observation to ligand-substrate halogen-π interactions^{40,42,43} within the C–C bond-forming transition structures as indicated by DFT calculations (*vide infra*).

Among the oxidants tested, feedstock chemical di-*tert*-butyl peroxide (*t*BuO)₂ provided the highest yield of **3a** while minimizing alkyne homocoupling compared to other oxidants commonly employed in cross-coupling reactions (entries 4–6, see also Table S2).^{19–21} We anticipate that the amine additive is crucial in facilitating the single-electron activation of

Table 1 Reaction Optimisation^a

Entry	Variation from standard conditions	Yield (%)	Er
1	None	83	91 : 9
2	CuI as copper source	46	90 : 10
3	Cu(CH ₃ CN) ₄ PF ₆ as copper source	44	88 : 12
4	(cumylo) ₂ as oxidant	38	90 : 10
5	PhI(OAc) ₂ as oxidant	0	—
6	<i>t</i> BuOOH as oxidant	0	—
7	DCM as solvent	56	88 : 12
8	PhCl as solvent	66	89 : 11
9	DMAP as additive	<5	—
10	4-Trifluoromethylaniline as additive	<5	—
11	4-Methoxyaniline as additive	70	90 : 10
12	No additive	0	—
13	23 °C	12	91 : 9
14	80 °C	58	89 : 11

Ligand optimization:



^a Reaction conditions unless otherwise noted: 4,4,5,5-tetramethyl-2-(1-phenylhexyl)-1,3,2-dioxaborolane (**1a**, 0.10 mmol), 2-ethynylthiophene (**2a**, 0.30 mmol), aniline (0.10 mmol), specified catalyst mixture, di-*tert*-butyl peroxide (0.30 mmol), and toluene (0.1 M); reaction yields were determined by ¹H NMR spectroscopy of the crude reaction mixture using 1,1,2,2-tetrachloroethane as an internal standard (see the SI for details). The enantiomeric ratio (er) of product **3a** was determined by chiral high-performance liquid chromatography (HPLC) analysis.

alkylboron reagents.^{34–36} A range of substituted anilines and alkylamines were tested, with the highest yield and enantioselectivity obtained using a stoichiometric amount of aniline (entries 9–12, see also Table S2). No C–N coupling was observed under the optimized reaction conditions. Reaction carried out in toluene (entries 7–8, Table S2) at 60 °C (entries 13–14) yielded the optimal result. An exogenous base was employed to promote the alkyne transmetalation step, with the best outcome achieved using Cs₂CO₃ (Table S2).

Substrate scope

With the optimized reaction conditions, we assessed the functional group tolerance and scope of compatible alkylboronic pinacol esters and alkynes (Fig. 2). The absolute configuration



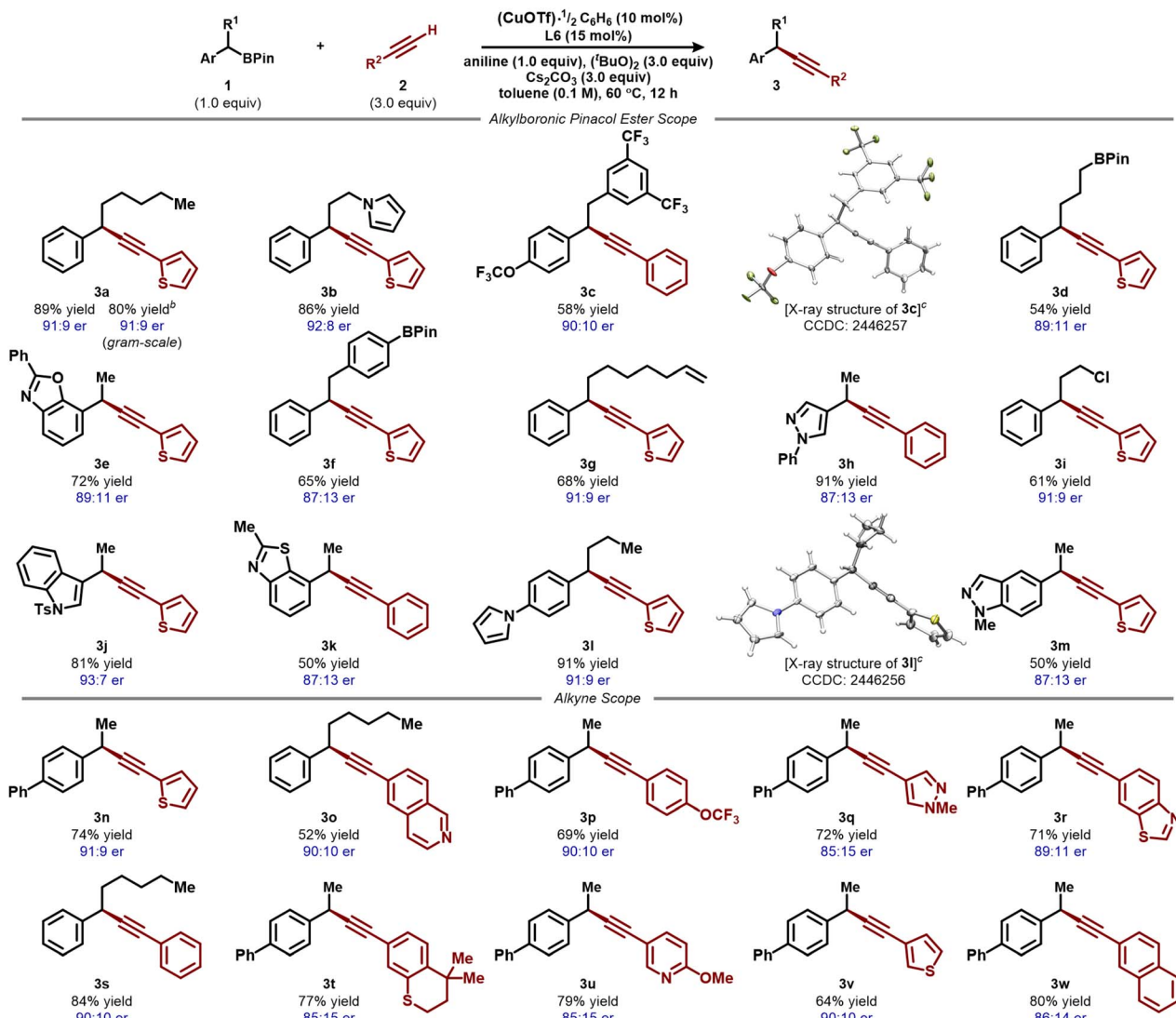


Fig. 2 Reaction Scopea (a) all yields were obtained using 0.50 mmol of alkylboronic pinacol ester substrates unless otherwise noted. Enantiomeric ratio (er) was determined by chiral HPLC analysis. (b) Reaction carried out on a 5.00 mmol scale of substrate **1a**. (c) Solid-state molecular structure of **3c** and **3l** with thermal ellipsoids at 50% probability level. Colour scheme: S, yellow; N, blue; C, grey; O, red; F, yellow-green; H, white.

of the major enantiomer was determined by a combination of optical rotation measurements and the solid-state structures of products **3c** and **3l**. The reaction proceeds effectively in the presence of various heterocycles commonly found in pharmaceuticals,^{44–47} including thiophene (**3a**), pyrrole (**3b**, **3l**), benzoxazole (**3e**), pyrazole (**3h**), indole (**3j**), benzothiazole (**3k**, **3r**), indazole (**3m**), isoquinoline (**3o**), thiochromane (**3t**), and pyridine (**3u**).

Functionalization of substrates containing aza-heterocycles (**3h**, **3m**, **3o**, **3q**, **3r**) proceeds effectively with no detectable side products resulting from radical addition. Functional groups prone to oxidation, such as thioether (**3t**), are tolerated under reaction conditions. The protocol is compatible with weak allylic (**3g**)/benzylic C–H bonds (**3c**, **3f**) and proceeds smoothly in the presence of alkyl halide (**3i**). These results highlight the orthogonality of the deborylative alkynylation approach to emerging catalytic strategies, such as asymmetric

C–H functionalization or Sonogashira-type transformations.^{22–30} The protocol exhibits high selectivity between different alkylboronic pinacol esters. For substrates containing additional aryl (**3f**) or primary alkyl boronic esters (**3d**), only the products resulting from benzylic functionalization were obtained. To further highlight the synthetic utility of the enantioconvergent alkynylation protocol, the synthesis of **3a** was carried out on a 5.0 mmol scale, resulting in comparable yield and enantioselectivity to the 0.5 mmol scale reactions.

Mechanistic investigation

Building on the successful application of the alkynylation protocol across a broad substrate scope, we integrated experimental and theoretical studies to elucidate the reaction mechanism and origin of enantioselectivity, with the goal of guiding future chiral ligand design and advancing the asymmetric



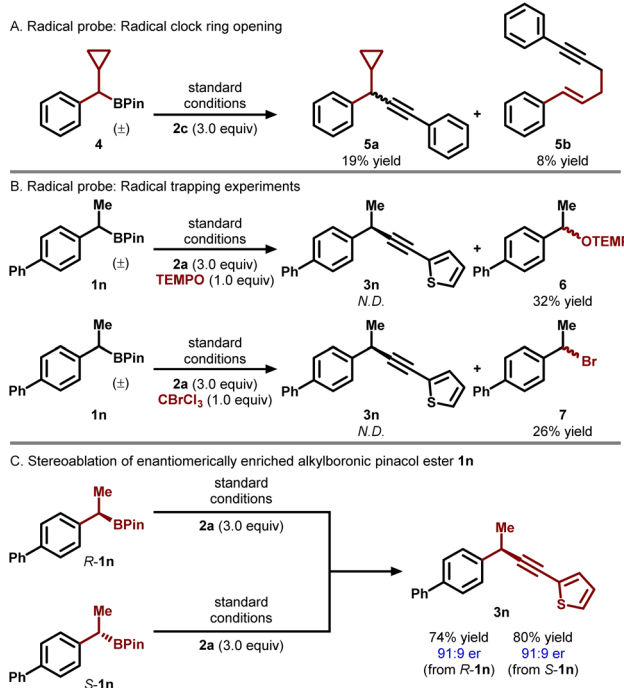


Fig. 3 Mechanistic probes for the asymmetric deborylative alkynylation (reactions were carried out on a 0.10 mmol scale. Yields were determined by ^1H NMR spectroscopy of the crude product mixture using 1,1,2,2-tetrachloroethane as an internal standard). (A) The proposed alkyl radical formation is supported by radical ring opening of the cyclopropyl substituent in substrate 4. (B) The alkyl radical intermediates can be intercepted using radical traps. (C) Stereochemical information is lost after the generation of an alkyl radical.

deborylative C–C cross-coupling platform. Alkylation of radical clock substrate 4 led to the formation of product 5a and ring-opened 5b, indicating the intermediacy of an alkyl radical (Fig. 3A). Radical trapping experiments were carried out using TEMPO and CBrCl_3 (Fig. 3B). In both cases, the formation of 3n was inhibited while the TEMPO-coupled product 6 and brominated product 7 were observed in 32% and 26% yield, respectively, supporting the involvement of an alkyl radical intermediate. Subjecting enantiomerically enriched *R*- or *S*-1n to the reaction conditions resulted in the generation of product 3n with a similar enantiomeric ratio favoring the same major enantiomer, indicating the loss of stereochemical information prior to C–C bond formation (Fig. 3C).

Computational studies were next carried out to investigate our proposed mechanism and elucidate the origins of enantioconvergence. Dispersion-corrected DFT calculations were performed at the B3LYP-D3(BJ)/def2-TZVP-SMD(toluene)//B3LYP-D3(BJ)/def2-SVP & def2-TZVP(Cu, Br)-SMD(toluene) level of theory.^{48–54} We modelled the coupling between alkylboronic pinacol ester 1n and 2-ethynylthiophene 2a with ligand L6 via an inner-sphere pathway.²² Our previous computational study³⁵ indicated that among several plausible C–B bond activation pathways, inner-sphere aminyl radical activation is kinetically most favourable. We propose that an analogous mechanistic framework underlies the alkynylation system. Control experiments (Table 1, entries 10–12) underscore the critical role of

aniline in this protocol. We hypothesized that substrate 1n undergoes aminyl-radical-mediated C–B bond cleavage: H-atom transfer between aniline and *tert*-butoxy radical generates the anilinyl radical (Fig. 1C), which in turn initiates C–B bond homolysis in 1n to produce alkyl radical 9· and ArNH-Bpin as a stoichiometric byproduct. (see SI, Scheme S1 and S2 for details).³⁵ Computational results (Fig. 4A) indicated that the addition of radical 9· to divalent Cu intermediate 8⁵⁵ is slightly endergonic, generating formal Cu(II) intermediates 10_R ($\Delta G = 1.7 \text{ kcal mol}^{-1}$) and 10_S ($\Delta G = 1.5 \text{ kcal mol}^{-1}$). The subsequent C–C bond formation proceeds *via* competing diastereomeric reductive elimination transition structures (TSs) TS1_R and TS1_S, with retention of configurations at the benzylic positions. While formation of 10_S is slightly favoured thermodynamically ($\Delta\Delta G = 0.2 \text{ kcal mol}^{-1}$), the *R*-enantiomer pathway is kinetically

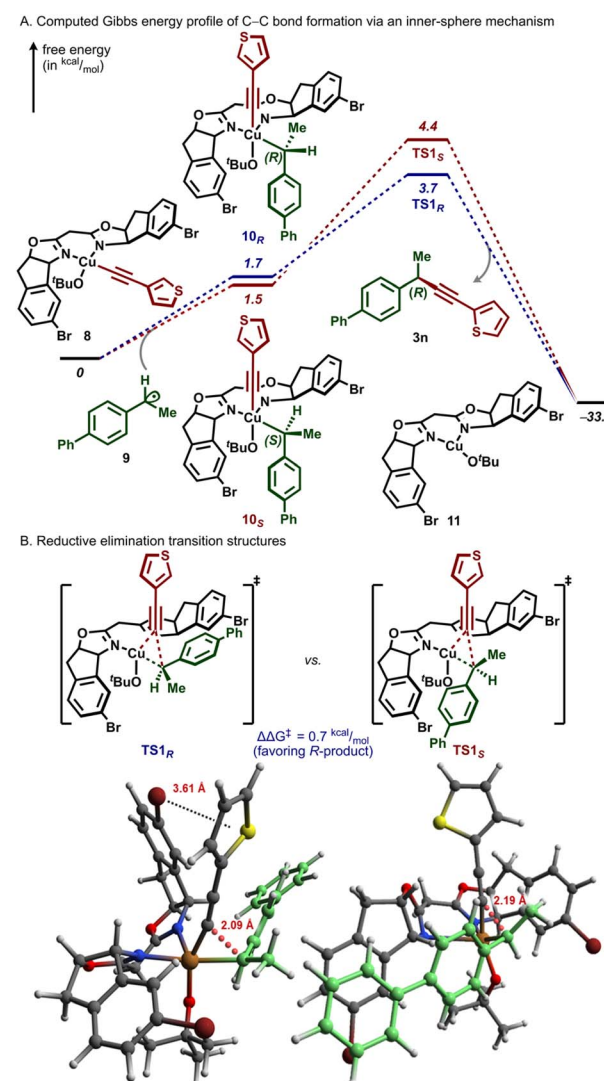


Fig. 4 Computational investigation into the C–C bond-forming mechanism. (A) Potential energy surface of alkynylation *via* an inner-sphere pathway. (B) Reductive elimination transition state structures reveal favourable non-covalent halogen– π interaction in TS1_R. (B3LYP-D3(BJ)/def2-TZVP-SMD(toluene)//B3LYP-D3(BJ)/def2-SVP-SMD(toluene)). Alkyl fragment is coloured green. The forming C–C bond is coloured red.



preferred ($\Delta\Delta G^\ddagger = 0.7$ kcal mol⁻¹, consistent with experimental observations), indicating that radical **9** capture is likely reversible and proceeds with a low barrier. Analysing the noncovalent interaction (NCI) isosurfaces of **TS1_R** and **TS1_S** attributes the selectivity to attractive ligand-substrate halogen- π interactions^{40,42,43} between a bromine substituent and an axial 2-thiopheneacetylide ligand (Fig. 4B). The bond metrics (Br-Ar(centroid) distance: 3.61 Å; C-Br-Ar(centroid) angle: 104.4°)⁵⁶ are consistent with halogen- π interactions observed in enzymatic systems, where aromatic side chains align to facilitate arene electron density donation to the σ -hole of the C-Br bond.^{42,57} Similar interaction is absent in **TS1_S** due to the opposing orientation of ligand Br substituent and the alkynyl group (Scheme S7).⁵⁸

Conclusions

In summary, we have developed a Cu-catalyzed enantioconvergent deborylative alkynylation protocol. This method is compatible with a wide range of functional groups and heterocycles. The alkynylation product can be obtained on a gram scale with good enantioselectivity. Mechanistic evidence suggests the generation of prochiral radicals in a stereoablativ fashion, followed by enantioselective radical trapping by Cu(II) intermediates. DFT calculation supports the viability of an inner-sphere mechanism and attributes the observed enantioselectivity to ligand-substrate halogen- π interactions.

Author contributions

YD conceptualized the work. JFH, YD, and BZ performed the experiments in this project. TJS carried out the computational work. YD, JFH, and TJS prepared the manuscript.

Conflicts of interest

There are no conflicts to declare.

Data availability

CCDC 2446256 and 2446257 contain the supplementary crystallographic data for this paper.^{59a,b}

All experimental procedures and data related to this study can be found in the SI. Supplementary information is available. See DOI: <https://doi.org/10.1039/d5sc04733a>.

Acknowledgements

This work was supported by startup funds from Colorado State University. We are grateful to Dr Robert S. Paton for advice on the computational study in this manuscript.

Notes and references

- 1 H. DeFrancesco, J. Dudley and A. Dudley, Boron Reagents in Synthesis, *Am. Chem. Soc.*, 2016, **1**–25.
- 2 J. W. B. Fyfe and A. J. B. Watson, Recent Developments in Organoboron Chemistry: Old Dogs, New Tricks, *Chem.*, 2017, **3**, 31–55.
- 3 E. Fernández, and A. Whiting, *Synthesis and Application of Organoboron Compounds*, Springer International Publishing, 2015.
- 4 X. Yang, S. J. Kalita, S. Maheshuni and Y.-Y. Huang, Recent advances on transition-metal-catalyzed asymmetric tandem reactions with organoboron reagents, *Coord. Chem. Rev.*, 2019, **392**, 35–48.
- 5 D. S. Matteson, *Stereodirected Synthesis with Organoboranes*, Springer Berlin Heidelberg, 2012.
- 6 B. S. L. Collins, C. M. Wilson, E. L. Myers and V. K. Aggarwal, Asymmetric Synthesis of Secondary and Tertiary Boronic Esters, *Angew. Chem., Int. Ed.*, 2017, **56**, 11700–11733.
- 7 S. P. Thomas, R. M. French, V. Jheengut and V. K. Aggarwal, Homologation and alkylation of boronic esters and boranes by 1,2-metallate rearrangement of boron ate complexes, *Chem. Record*, 2009, **9**, 24–39.
- 8 J. W. Lehmann, D. J. Blair and M. D. Burke, Towards the generalized iterative synthesis of small molecules, *Nat. Rev. Chem.*, 2018, **2**, 0115.
- 9 H. Wang, C. Jing, A. Noble and V. K. Aggarwal, Stereospecific 1,2-Migrations of Boronate Complexes Induced by Electrophiles, *Angew. Chem., Int. Ed.*, 2020, **59**, 16859–16872.
- 10 T. Klis, S. Lulinski and J. Serwatowski, Formation and Synthetic Applications of Metalated Organoboranes, *Curr. Org. Chem.*, 2010, **14**, 2549–2566.
- 11 I. Marek and J.-F. Normant, Synthesis and Reactivity of sp³-Geminated Organodimetallics, *Chem. Rev.*, 1996, **96**, 3241–3268.
- 12 K. Hong, X. Liu and J. P. Morken, Simple Access to Elusive α -Boryl Carbanions and Their Alkylation: An Umpolung Construction for Organic Synthesis, *J. Am. Chem. Soc.*, 2014, **136**, 10581–10584.
- 13 R. Nallagonda and R. R. Karimov, Copper-Catalyzed Regio- and Diastereoselective Additions of Boron-Stabilized Carbanions to Heteroarenium Salts: Synthesis of Azaheterocycles Containing Contiguous Stereocenters, *ACS Catal.*, 2021, **11**, 248–254.
- 14 B. Lee and P. J. Chirik, Ketone Synthesis from Benzylboronates and Esters: Leveraging α -Boryl Carbanions for Carbon–Carbon Bond Formation, *J. Am. Chem. Soc.*, 2020, **142**, 2429–2437.
- 15 H. Jin, J. Han, X. Liu, C. Feng and M. Zhan, Access to Diverse Organoborons by α -Deprotonation and Functionalization of Benzylboronates, *Org. Lett.*, 2023, **25**, 4168–4172.
- 16 J. F. Hartwig, *Organotransition Metal Chemistry: From Bonding to Catalysis*, University Science Books, 2010.
- 17 Y. Wang, A. Noble, E. L. Myers and V. K. Aggarwal, Enantiospecific Alkynylation of Alkylboronic Esters, *Angew. Chem., Int. Ed.*, 2016, **55**, 4270–4274.
- 18 N. Xu, H. Liang and J. P. Morken, Copper-Catalyzed Stereospecific Transformations of Alkylboronic Esters, *J. Am. Chem. Soc.*, 2022, **144**, 11546–11552.
- 19 D. L. Golden, S.-E. Suh and S. S. Stahl, Radical C(sp³)-H functionalization and cross-coupling reactions, *Nat. Rev. Chem.*, 2022, **6**, 405–427.



20 F. Wang, P. Chen and G. Liu, Copper-Catalyzed Radical Relay for Asymmetric Radical Transformations, *Acc. Chem. Res.*, 2018, **51**, 2036–2046.

21 Z. Zhang, P. Chen and G. Liu, Copper-catalyzed radical relay in C(sp³)-H functionalization, *Chem. Soc. Rev.*, 2022, **51**, 1640–1658.

22 L. Fu, Z. Zhang, P. Chen, Z. Lin and G. Liu, Enantioselective Copper-Catalyzed Alkynylation of Benzylic C–H Bonds via Radical Relay, *J. Am. Chem. Soc.*, 2020, **142**, 12493–12500.

23 L. Fu, S. Zhou, X. Wan, P. Chen and G. Liu, Enantioselective Trifluoromethylalkynylation of Alkenes via Copper-Catalyzed Radical Relay, *J. Am. Chem. Soc.*, 2018, **140**, 10965–10969.

24 H.-D. Xia, Z.-L. Li, Q.-S. Gu, X.-Y. Dong, J.-H. Fang, X.-Y. Du, L.-L. Wang and X.-Y. Liu, Photoinduced Copper-Catalyzed Asymmetric Decarboxylative Alkynylation with Terminal Alkynes, *Angew. Chem., Int. Ed.*, 2020, **59**, 16926–16932.

25 X.-Y. Dong, Y.-F. Zhang, C.-L. Ma, Q.-S. Gu, F.-L. Wang, Z.-L. Li, S.-P. Jiang and X.-Y. Liu, A general asymmetric copper-catalysed Sonogashira C(sp³)-C(sp) coupling, *Nature Chem.*, 2019, **11**, 1158–1166.

26 G. Lei, H. Zhang, B. Chen, M. Xu and G. Zhang, Copper-catalyzed enantioselective arylalkynylation of alkenes, *Chem. Sci.*, 2020, **11**, 1623–1628.

27 X. Mo, R. Guo and G. Zhang, Recent Developments in Copper(I)-Catalyzed Enantioselective Alkynylation Reactions via a Radical Process, *Chin. J. Chem.*, 2023, **41**, 481–489.

28 Y. Zhang, Y. Sun, B. Chen, M. Xu, C. Li, D. Zhang and G. Zhang, Copper-Catalyzed Photoinduced Enantioselective Dual Carbofunctionalization of Alkenes, *Org. Lett.*, 2020, **22**, 1490–1494.

29 X.-Y. Dong, J.-T. Cheng, Y.-F. Zhang, Z.-L. Li, T.-Y. Zhan, J.-J. Chen, F.-L. Wang, N.-Y. Yang, L. Ye, Q.-S. Gu and X.-Y. Liu, Copper-Catalyzed Asymmetric Radical 1,2-Carboalkynylation of Alkenes with Alkyl Halides and Terminal Alkynes, *J. Am. Chem. Soc.*, 2020, **142**, 9501–9509.

30 J. Li, L. Ning, Q. Tan, X. Feng and X. Liu, Asymmetric Sonogashira C(sp³)-C(sp) bond coupling enabled by a copper(I) complex of a new guanidine-hybrid ligand, *Org. Chem. Front.*, 2022, **9**, 6312–6318.

31 A. Bakhoda, O. E. Okoromoba, C. Greene, M. R. Boroujeni, J. A. Bertke and T. H. Warren, Three-Coordinate Copper(II) Alkynyl Complex in C–C Bond Formation: The Sesquicentennial of the Glaser Coupling, *J. Am. Chem. Soc.*, 2020, **142**, 18483–18490.

32 C. Ollivier and P. Renaud, Organoboranes as a Source of Radicals, *Chem. Rev.*, 2001, **101**, 3415–3434.

33 P. Renaud, A. Beauseigneur, A. Brecht-Forster, B. Becattini, V. Darmency, S. Kandhasamy, F. Montermini, C. Ollivier, P. Panchaud, D. Pozzi, E. M. Scanlan, A.-P. Schaffner and V. Weber, Boron: A key element in radical reactions, *Pure Appl. Chem.*, 2007, **79**, 223–233.

34 Z. Wang, N. Wierich, J. Zhang, C. G. Daniliuc and A. Studer, Alkyl Radical Generation from Alkylboronic Pinacol Esters through Substitution with Aminyl Radicals, *J. Am. Chem. Soc.*, 2023, **145**, 8770–8775.

35 J. Vu, G. C. Haug, Y. Li, B. Zhao, C. J. Chang, R. S. Paton and Y. Dong, Enantioconvergent Cross-Nucleophile Coupling: Copper-Catalyzed Deborylative Cyanation, *Angew. Chem., Int. Ed.*, 2024, **63**, e202408745.

36 C. Zhu, J. Lin, X. Bao and J. Wu, Development of N-centered radical scavengers that enables photoredox-catalyzed transition-metal-free radical amination of alkyl pinacol boronates, *Nat. Commun.*, 2025, **16**, 3225.

37 I. W. Davies, R. J. Deeth, R. D. Larsen and P. J. Reider, A CLFSE/MM study on the role of ligand bite-angle in Cu(II)-catalyzed Diels-Alder reactions, *Tetrahedron Lett.*, 1999, **40**, 1233–1236.

38 R. S. J. Proctor, A. C. Colgan and R. J. Phipps, Exploiting attractive non-covalent interactions for the enantioselective catalysis of reactions involving radical intermediates, *Nature Chem.*, 2020, **12**, 990–1004.

39 G. Lu, R. Y. Liu, Y. Yang, C. Fang, D. S. Lambrecht, S. L. Buchwald and P. Liu, Ligand–Substrate Dispersion Facilitates the Copper-Catalyzed Hydroamination of Unactivated Olefins, *J. Am. Chem. Soc.*, 2017, **139**, 16548–16555.

40 S. Jiang, L. Zhang, D. Cui, Z. Yao, B. Gao, J. Lin and D. Wei, The Important Role of Halogen Bond in Substrate Selectivity of Enzymatic Catalysis, *Sci. Rep.*, 2016, **6**, 34750.

41 Another interpretation of the results involves the deprotonation of meso-hydrogen to generate an anionic BOX ligand. We tested this hypothesis by subjecting a mixture of ligand **L6**, Cu source, and Cs₂CO₃ to reaction conditions. No deprotonation of the ligand **L6** was observed by ¹H NMR spectroscopy.

42 M. B. Shah, J. Liu, Q. Zhang, C. D. Stout and J. R. Halpert, Halogen–π Interactions in the Cytochrome P450 Active Site: Structural Insights into Human CYP2B6 Substrate Selectivity, *ACS Chem. Biol.*, 2017, **12**, 1204–1210.

43 J. Jian, J. Poater, P. B. White, C. J. McKenzie, F. M. Bickelhaupt and J. Mecinović, Probing Halogen–π versus CH–π Interactions in Molecular Balance, *Org. Lett.*, 2020, **22**, 7870–7873.

44 J. Jampilek, Heterocycles in Medicinal Chemistry, *Molecules*, 2019, **24**, 3839.

45 M. M. Heravi and V. Zadsirjan, Prescribed drugs containing nitrogen heterocycles: an overview, *RSC Adv.*, 2020, **10**, 44247–44311.

46 R. D. Taylor, M. MacCoss and A. D. G. Lawson, Rings in Drugs, *J. Med. Chem.*, 2014, **57**, 5845–5859.

47 J. J. Rojas and J. A. Bull, Oxetanes in Drug Discovery Campaigns, *J. Med. Chem.*, 2023, **66**, 12697–12709.

48 A. D. Becke, Density-functional thermochemistry. III. The role of exact exchange, *J. Chem. Phys.*, 1993, **98**, 5648–5652.

49 C. Lee, W. Yang and R. G. Parr, Development of the Colle-Salvetti correlation-energy formula into a functional of the electron density, *Phys. Rev. B: Condens. Matter Mater. Phys.*, 1988, **37**, 785–789.

50 P. J. Stephens, F. J. Devlin, C. F. Chabalowski and M. J. Frisch, *Ab Initio* Calculation of Vibrational Absorption and Circular Dichroism Spectra Using Density Functional Force Fields, *J. Phys. Chem.*, 1994, **98**, 11623–11627.



51 S. H. Vosko, L. Wilk and M. Nusair, Accurate spin-dependent electron liquid correlation energies for local spin density calculations: a critical analysis, *Can. J. Phys.*, 1980, **58**, 1200–1211.

52 F. Weigend and R. Ahlrichs, Balanced basis sets of split valence, triple zeta valence and quadruple zeta valence quality for H to Rn: Design and assessment of accuracy, *Phys. Chem. Chem. Phys.*, 2005, **7**, 3297–3305.

53 F. Weigend, Accurate Coulomb-fitting basis sets for H to Rn, *Phys. Chem. Chem. Phys.*, 2006, **8**, 1057–1065.

54 F. Neese, F. Wennmohs, U. Becker and C. Ripplinger, The ORCA quantum chemistry program package, *J. Chem. Phys.*, 2020, **152**, 224108.

55 Initial oxidation of Cu(I) alkynyl intermediate with (⁷BuO)₂ is exergonic (−0.9 kcal mol^{−1}), resulting in the formation of divalent complex **8** (Scheme S3).

56 The deviation from linearity weakens the interaction and likely underlies the modest enantioselectivity observed experimentally.

57 Y. Lu, Y. Wang and W. Zhu, Nonbonding interactions of organic halogens in biological systems: implications for drug discovery and biomolecular design, *Phys. Chem. Chem. Phys.*, 2010, **12**, 4543–4551.

58 Consistent with our model, low to moderate levels of enantioselectivity were observed in coupling reactions with alkynes bearing electron-deficient arenes and alkyl groups. (Table S3) Although substrate **3o** containing isoquinoline was obtained with good enantioselectivity, the electron-withdrawing aza-group is not incorporated in the arene directly engaging in Br–π attraction.

59 (a) J. F. Head, T. J. Schubert, B. Zhao, Y. Dong, CCDC 2446256, Experimental Crystal Structure Determination, 2025, DOI: [10.5517/ccdc.csd.cc2n3jht](https://doi.org/10.5517/ccdc.csd.cc2n3jht); (b) J. F. Head, T. J. Schubert, B. Zhao, Y. Dong, CCDC 2446257, Experimental Crystal Structure Determination, 2025, DOI: [10.5517/ccdc.csd.cc2n3jjv](https://doi.org/10.5517/ccdc.csd.cc2n3jjv).

